A priori evaluation of the solvent contribution to the reorganization energy accompanying intramolecular electron transfer: Predicting the nature of the Creutz Taube ion

ARTICLE *in* CHEMICAL PHYSICS · DECEMBER 2005

Impact Factor: 1.65 · DOI: 10.1016/j.chemphys.2005.06.039

3 AUTHORS:

Jeffrey Reimers
University of Technology Sydney
215 PUBLICATIONS **6,671** CITATIONS
SEE PROFILE

Zheng-Li Cai
University of Sydney
37 PUBLICATIONS **1,160** CITATIONS
SEE PROFILE

Noel Hush
University of Sydney
309 PUBLICATIONS **11,594** CITATIONS
SEE PROFILE

Available online at www.sciencedirect.com
SCIENCE DIRECT®
Chemical Physics 319 (2005) 39–51
Chemical Physics
www.elsevier.com/locate/chemphys

A priori evaluation of the solvent contribution to the reorganization energy accompanying intramolecular electron transfer: Predicting the nature of the Creutz–Taube ion

Jeffrey R. Reimers [a,*], Zheng-Li Cai [a], Noel S. Hush [a,b]

[a] School of Chemistry, The University of Sydney, NSW 2006, Australia
[b] School of Molecular and Microbial Biosciences, The University of Sydney, NSW 2006, Australia

Received 7 January 2005; accepted 15 June 2005
Available online 8 August 2005

Abstract

The solvent contribution to the reorganization energy is one of the key physical properties controlling electron-transfer processes. A priori computational schemes have been developed that can predict realistic values for all other properties controlling charge transfer such as electronic couplings, vibronic couplings for intramolecular modes, the effects of asymmetry, and the effects of symmetric modes, but robust schemes for treating solvation remain elusive. In recent years, excited-state quantum chemical electronic-structure packages have gained the ability to calculate non-equilibrium solvation effects without the need to treat solvent explicitly, establishing the core of the required technology. While quantum chemical schemes involving excited-states represented as perturbed ground states can readily be applied in such calculations, they in general fail to include sufficient inactive-electron correlation to properly describe the excited-state manifold of charge transfer states, states for which only multi-reference procedures may robustly be applied. We develop computational procedures by which complete-active-space self-consistent-field (CASSCF) and related multi-reference calculations may be applied to electron-transfer systems whose energetics are controlled by the solvent–solute interaction. This is tested through the evaluation of the reorganization energy for electron-transfer in the bis-pentaammineruthenium complexes of α,ω-dipyridyl *trans*-polyenes in aqueous solution. Predictions are then made for the Creutz–Taube ion that place it clearly in the region of maximum breakdown of the Born–Oppenheimer approximation for which both the localized and delocalized diabatic descriptions of its electronic structure become inappropriate. This result is in qualitative agreement with conclusions drawn over the last four years based on a number of sources.

Keywords: Solvent reorganization energy; Multi-reference; Intervalence charge transfer; Creutz–Taube ion; Non-Condon effects; Symmetric modes

1. Introduction

Electron transfer processes are thought of as taking place in donor-bridge-acceptor (DBA) systems in which an electron leaves the donor (D), tunnels through the bridge (B) and arrives at the acceptor (A). While both intermolecular and intramolecular processes of this type are extremely important biochemically, much fundamental knowledge has been gained through the examination of simple model chemical systems in which covalent bonding is used to restrict the atomic structure and hence expose the intrinsic electronic processes. Key inorganic molecules designed for this purpose include the Creutz–Taube ion [1,2] **1** and the related bis-pentaammineruthenium complexes of α,ω-dipyridyl *trans*-polyenes [3–5] **2**–**4**; these are symmetric systems in which the donor and acceptor moieties, d_π orbitals on the ruthenium centres, are the same. For these compounds, the interesting oxidation state is the 5+ state with one

* Corresponding author.
E-mail address: reimers@chem.usyd.edu.au (J.R. Reimers).

0301-0104/$ - see front matter © 2005 Elsevier B.V. All rights reserved.
doi:10.1016/j.chemphys.2005.06.039

electron hole present in the otherwise filled t_{2g} sub-shells of the metal atoms. Understanding of the location and motion of this hole is a significant conceptual challenge as the Born–Oppenheimer adiabatic approximation [6] that forms the basis for almost all chemical understanding is not applicable. It is this approximation that separates nuclear and electronic motions, allowing "atoms" to be identified within molecules that would otherwise need to be treated as a plasma of strongly interacting positive and negative electrical charges. Basically, the motion of the electron hole becomes coupled to the nuclear motions in a process known as *vibronic coupling* [7]. Approaching either of two limits, the Born–Oppenheimer approximation becomes again valid, allowing normal chemical identities to be assigned to the DBA system: these are the *localized diabatic* approximation in which the hole is localized on one metal, producing an asymmetric Ru(II)–Ru(III) mixed-valence species, and the *delocalized diabatic* limit in which the hole is delocalized over both metals forming an effective long-range bridge-mediated covalent bond between them. In between the two diabatic limits is the strongly non-adiabatic one in which the notion of a molecular potential-energy surface becomes meaningless.

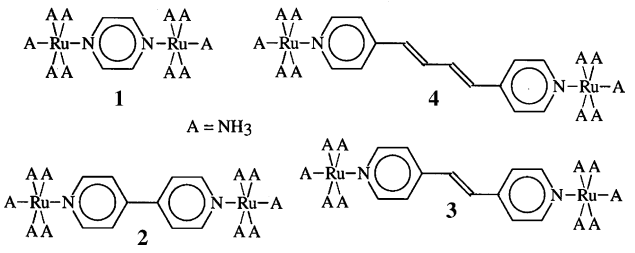

All electron-transfer processes raise the same general conceptual issues of understanding, though most biochemical scenarios, for example, involve the localized diabatic limit in which the kinetics and spectroscopy are simply described. The basic physical properties such as the electronic coupling and the electron–phonon interaction have vastly different manifestations in the various adiabatic and non-adiabatic limits, however. Our interests are in the development of robust computational methods that can predict reliable values for these properties a priori [8–15] and the development of computational tools that can predict experimental results from these properties *independent* of the nature of the vibronic coupling [16–21]. So far, a priori computational methods are readily available for all key properties except the solvent contribution to the reorganization energy for intramolecular charge-transfer spectroscopy. Previously, we [22,23] and others [24–29] have developed methods for the treatment of problems involving specific solvation effects requiring explicit knowledge of the liquid structure, but this level of effort is not required for most problems [30] and may not be necessary for the Creutz–Taube ion and related systems. The establishment of a simple a priori method based on the alternate use of dielectric-continuum representations of the solvent is the focus of this work.

In principle, a charge-transfer absorption band is no different from any other spectroscopic transition. A priori dielectric-continuum based methods have been developed to evaluate the solvent effect on transition energies [31–34], and Kuznetsov was one of the first researchers to apply these methods to calculate solvent reorganization energies [33]. However, intramolecular charge-transfer processes are intrinsically associated with large scale rearrangements of the spectator electrons not involved in the electron transfer, an effect that typically demands the application of specialised electronic-structure computational techniques. Computational methods such as configuration-interaction singles (CIS) and time-dependent density-functional theory (TD-DFT) use single-reference starting points that bias the calculations strongly in favour of non-charge-transfer states and hence, in general, predict poor excited-state manifolds; the use of multi-reference computational methods is thus essential in order to treat all states of interest on an equal footing [22,35]. Also, solvation may totally change the electronic structure of the system, making gas-phase geometries inappropriate for use in evaluating the solvent reorganization energy. What is developed herein is a robust means for the application of existing multi-reference electronic-structure methods for evaluating non-equilibrium solvation effects on spectral transition energies to study intramolecular charge-transfer transitions. This strategy takes into account systems with solvent–chromophore interaction that are sufficiently strong to determine the ordering of the key states, as well as taking into account systems displaying large non-Condon effects associated with intramolecular displacements in symmetric vibrational modes.

The importance of the medium to charge-transfer phenomena is manifest in the Born solvation expression [36] according to which the solvation energy of an ion increases quadratically with the magnitude of its charge, hence strongly favouring charge-localized over charge-delocalized systems. For intermolecular charge transfer processes in which donor and acceptor can be considered to be infinitely separated, modern electronic-structure computational schemes based on self-consistent reaction-field (SCRF) models can be used quantitatively to calculate this effect. These adopt generalizations of the Born equation that place the molecules in appropriately shaped arbitrary solvent cavities rather than in the spherical cavity envisaged originally. For intramolecular processes as well as intermolecular ones in which the separation of the donor and acceptor is small compared to the individual extents, this process can no longer be thought of as comprising independent reduction and

oxidation processes but rather is one that involves rearrangement of an internal system dipole, requiring a more detailed approach. If the size of the chromophores dramatically exceeds their spacing, the simplest analytical model for the process becomes the Onsager equation [37] for the solvation of a molecular dipole in a spherical dielectric cavity. The dielectric response of a solvent is made up of two parts, however: an essentially instantaneous contribution arising from the electronic polarizability of the material, and a slow response, deemed too slow to occur on the timescale of electronic spectroscopy, associated with re-orientation of the dipole moments of the solvent molecules. The total response forming the external solvent reorganization energy λ_e is thus determined by both the static dielectric constant ϵ, and the high-frequency dielectric response n^2, where n is the refractive index of the material, and is given by [38–41]

$$\lambda_e = -\frac{2\epsilon - 2}{2\epsilon + 1}\frac{1}{r^3}\boldsymbol{\mu}\cdot\Delta\boldsymbol{\mu} - \frac{n^2-1}{2n^2+1}\frac{1}{r^3}\,|\,\Delta\boldsymbol{\mu}|^2, \tag{1}$$

where r is the cavity radius, $\boldsymbol{\mu}$ the initial value of the system dipole moment, and $\Delta\boldsymbol{\mu}$ the change in dipole accompanying charge transfer. For the intermediate case in which the donor and acceptor, treated as forming cavities of radii r_D and r_A, respectively, located a distance R apart ($R \gg r_D$ and r_A) is given by [42,43]

$$\lambda_e = \frac{e^2}{2}\left(\frac{1}{r_D} + \frac{1}{r_A} - \frac{2}{R}\right)\left(\frac{1}{n^2} - \frac{1}{\epsilon}\right), \tag{2}$$

where e is the magnitude of the charge on the electron.

Development of an a priori SCRF-based computational scheme will produce a method that is not only capable of interpolating between these two analytical limits but can also incorporate deviations from spherical shape of the individual donor and acceptor groups, account for the molecular nature of the bridging material, account for solvation of the bridge [44], account for the polarizability of the solute [22,28,33,45] and properly account for the interference terms between the two sources of electrical polarization that are included in Eq. (1) but excluded in Eq. (2) [24,46]. A wide variety of computational chemistry packages, including GAUSSIAN-03 [47], now support the calculation of non-equilibrium solvation effects arising from rapid electronic transitions occurring in a dielectric medium for molecules in arbitrarily shaped solvent cavities. We use the MOLCAS package [48] as it is designed specially for high-level calculations of molecular spectroscopic properties.

The application of such packages to evaluate the quantities of interest is not straightforward, however. Quantum-chemical codes operate strictly within the Born–Oppenheimer adiabatic approximation, returning an electronic structure for each requested nuclear structure. Hence the calculated electronic transition energies involve convolutions of the key physical properties such as the solvent contribution to the reorganization energy λ_e, just as do experimental observations. Thus computations must be poised so as to allow for the interpretation of their results in terms of simple quantities in much the same way as experiments in the field of electron transfer are designed. In effect, λ_e is a property of the system in its localized diabatic limit, the hypothetical limit in which the coupling between the two redox centres is completely eliminated. A variety of approaches may be used in order to produce the desired quantities including standard orbital localization schemes, schemes based on orbital overlap [49,50], schemes based on diagonalizing operators such as the dipole moment [16,51], or schemes based on fitting the shapes of the adiabatic potential-energy surfaces [52]. Herein, the approach taken is one of minimization of any possible effect produced by the method used for diabatization. This exploits chemical properties of the system being considered, electron transfer processes involving ruthenium d_π orbitals.

The method that we develop is tested by demonstrating that it quantitatively predicts the changes to the intervalence band maximum [53,54] that occurs on increasing the length of the central polyene chain in the bis-pentaammineruthenium complexes of α,ω-dipyridyl *trans*-polyenes [3–5]. Both experimentally and computationally, the results for this system are easy to interpret as the localized diabatic limit to the vibronic coupling is quite appropriate. Our method is then applied to interpret the properties of the Creutz–Taube ion [1,2], a possibly worst-case scenario [55–57] of considerable complexity for which not all significant issues have been resolved even after 35 years of intensive research.

The major issues concerning the nature of the Creutz–Taube ion have been recently reviewed [57], and the salient features may be summarized as follows. First, X-ray crystallographic data [58] indicate that the ion in its 5+ oxidation state is highly symmetric, suggesting a delocalized structure, even though tiny deviations from full symmetry are sometimes seen in asymmetric crystal environments. These results in effect provide an upper bound to the height of a possible double-well potential-energy surface: the two minima in such a surface pertain to localized Ru(II)–Ru(III) or Ru(III)–Ru(II) states, and the X-ray experiments indicate that, if a double well in fact exists, then the isomerization rate at the temperature of the experiment must be very rapid. The observation of single vibrational lines for many vibrational modes [2,59–61] at frequencies mid-way between those expected for Ru(II) and Ru(III) species indicates that the structure is delocalized on the ca. 3 ps timescale. Again, these results do not eliminate the possibility that tunnelling processes on the fs timescale occur between localized structures. However, key infrared absorptions arising from such tunnelling motions have never been

observed, despite considerable search [62]. All of these features thus suggest that the Creutz–Taube ion is fully charge delocalized on the shortest-accessible chemical timescale. However, some other key infrared and Raman transitions that are formally forbidden for the symmetric delocalized species have been unexpectedly observed [61,63,64]. These observations are indicative of vestigial localized character to the ion [55], and no quantitative analysis of the observed effects has been presented in terms of an intrinsically delocalized nature.

Quantitatively, the observed data has been interpreted in terms of the total reorganization energy involved in antisymmetric modes λ, a quantity that arises as the sum of the external solvent reorganization energy λ_e and the internal reorganization energy in intramolecular antisymmetric vibrational modes, λ_a, and the effective coupling J between the appropriate metal orbitals. If the effects of symmetric modes are ignored, as is usually assumed to be generally appropriate, then for $2|J|/\lambda \gg 1$ the system is in the delocalized adiabatic limit whilst for $2|J|/\lambda \ll 1$ it is in the localized diabatic limit [65]. The key parameters $|J|$and λ are usually extracted from the experimental data using analytical equations [54,66] derived using the Born–Oppenheimer adiabatic approximation, an approximation that works well in the two diabatic limits but which fails [16] in the non-adiabatic limit $2|J|/\lambda \sim 1$. From the temperature dependence of the absorption band of the Creutz–Taube ion, a value of $2|J|/\lambda = 1.7$ is obtained [59]; a similar value is also obtained from the observed absorption band width, once proper treatment of the contributions to the bandshape from symmetric modes is included in the analysis [67]. Unfortunately, values of this order depict a scenario too close to the non-adiabatic limit for the equations used to be quantitatively reliable [16]. Adiabatic equations remain in common use for the interpretation of systems in the non-adiabatic region [56], however, and so the original conclusion [59,67] that the Creutz–Taube ion is dominated by the effects of delocalization (whilst being near the intermediate non-adiabatic region between delocalized-dominated and localized dominated) is expected to remain valid. Qualitatively, the near independence on solvent observed for the intervalence absorption band, as well the observed dramatic change in shape with the introduction of asymmetry [68,69], support this analysis, but the effects appear to be too severe for $2|J|/\lambda \sim 1.7$. Proper quantitative treatment of all of these properties, as well as other very important ones such as the dependence of the absorption bandshape on solvation, requires full numerical simulation of the non-adiabatic coupling problem, taking proper account of the effects of the intramolecular symmetric and antisymmetric vibrational modes, the electronic coupling, the effects of solvation [8,16–18], and the effects of strongly interacting electronic states [70,71] that make the definition of a single effective coupling J somewhat ambiguous [19,20,72]. Perhaps the strongest evidence indicating charge delocalization in the Creutz–Taube ion has been the Stark spectroscopic data of Oh and Boxer [73,74] which, according to standard Born–Oppenheimer–Liptay analysis, contains no indication of localized character, but even the interpretation of this data must be made subject to non-adiabatic analysis for the true extent of any localized character to be revealed [18,21,75,76].

This discussion highlights not only the need for independent a priori estimates of the main properties such as the electronic coupling, the intramolecular symmetric and antisymmetric reorganization energies and distributions, and the external solvent reorganization energy λ_e, but also the need for a computational scheme that properly isolates these properties using adiabatic-based quantum-chemical electronic-structure calculations. While the need to properly treat symmetric modes in quantitative studies is well known [67], the central qualitative role of these modes in the process, via both direct modulation of the coupling and via contributions from interacting metal to ligand charge-transfer states [70,71] has only recently been recognized. Unexpected, non-Condon effects associated with large variations of calculated couplings J with molecular structure have been found [77]; in Section 4 we show that these are largely associated with changes in the ruthenium to bridge bond length. While this structural dependence is very significant for conceptual understanding of the properties of the system, it was discovered merely through consideration of the technical question of what is the most appropriate geometry to use in a priori calculations of J; with the aid of a full theory for the inclusion of the symmetric modes in the vibronic coupling problem [8,16,17], we have shown that $2J$ is most properly given as the difference in the adiabatic potential-energy minima of the ground and excited states, allowing a proper separation of the effects of the electronic coupling and the symmetric modes to be completed. Here, we seek a similar separation of the solvent reorganization energy contribution from the other system properties.

2. General computational approach

Previously [78] we have outlined and implemented a computational strategy for the a priori evaluation of most of the parameters (intramolecular vibrational frequencies, displacements, and vibronic coupling constants, as well as the electronic coupling) involved in non-adiabatic charge-transfer processes in large (pseudo-symmetric) DBA systems, the exception being the evaluation of the magnitude and influences of external solvent reorganization energy λ_a. This procedure is sketched in Fig. 1 and involves:

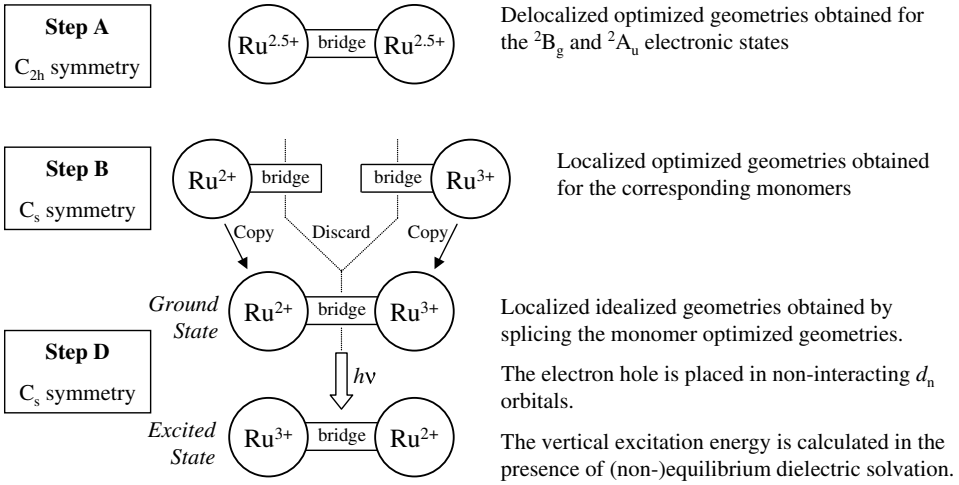

Fig. 1. Overview of the computational procedure.

Step A: evaluation of the adiabatic minimum-energy structures confined to high symmetry (C_{2h} in this work) for the two delocalized diabatic states (^2B_g and ^2A_u herein). The difference between the adiabatic energies of these structures is the coupling $2|J|$ whilst the energy differences between the vertically excited high-symmetry structures gives the symmetric-mode reorganization energy λ_s. If required, the contributions to λ_s from each individual mode can be determined by projecting (possibly using curvilinear coordinates [79]) the geometrical displacement between the two optimized diabatic states onto the normal modes of the molecule. From these calculations, the relative magnitudes of the vibronic coupling constants for each antisymmetric mode may also be evaluated, if required, from the vibronically induced infrared transition moments using the Herzberg–Teller equation [80]. An alternative to obtaining the vibronic coupling constants in this fashion is to optimize the structure of the localized diabatic states using a diabatization scheme such as the "Generalized Mulliken-Hush" (GMH) method of Cave and Newton [51], and then convert the vibrationally resolved Franck–Condon displacements so produced into vibronic coupling constants [8,16,17].

Step B: adiabatic geometry optimizations are performed for the appropriate monomer fragments (e.g. $Ru(NH_3)_5$-pyrazine for the Creutz–Taube ion) in low symmetry (C_s) for all accessed ionization states (ie., Ru(II) and Ru(III)). The sum of the vertical excitation energies for the oxidation and reduction processes gives the total internal reorganization energy $\lambda = \lambda_a + \lambda_s$.

Step C: the antisymmetric-mode internal reorganization energy λ_a is determined from the difference between λ evaluated in Step B and λ_s evaluated in Step A. Also, the absolute magnitude of all of the vibronic coupling constants can be determined once λ_a is known.

This method was previously employed to determine the nature of the hole-transport process within the "special pair" of chlorophyll-like molecules that are responsible for primary charge separation during photosynthesis [78], a problem for which 50 antisymmetric modes and 20 symmetric modes are required in the vibronic coupling model in order to describe the observed spectroscopic and chemical properties of the system [8,18], but a system in which the effect of the surrounding environment does not significantly modify the intramolecular properties. In Section 4, we demonstrate that this result does not apply for inorganic complexes with centres of high charge density through the completion of geometry optimizations both with and without the presence of solvent. The dependence of the intramolecular geometry on the solvent raises the question as to whether or not solvent-corrected energies should be used in the evaluation of J, λ_a, and λ_s, etc. during Steps A–C. Solvent-corrected energies would appear to be the most appropriate ones and we determine λ_s in this fashion, making it no longer a purely intramolecular quantity. Analogous determination of λ_a is not possible, however, as the procedure used in Step B of adding the reorganization energies for oxidation and reduction of each monomer fragment would implicitly double-count the contributions from regions of the solvent that are accessible to both chromophores; in reality the effects of these regions should cancel rather than add, reducing in the limit of spherical moieties the independent-species Born equation approach to the Onsager equation. Hence only gas-phase energies may be used in Step B, and the solvent contribution to the reorganization energy is not accessible using this means.

To determine λ_e we introduce *Step D* and perform calculations of the full dimeric system at an idealized, fully charge-localized, low-symmetry geometry. This geometry is obtained by splicing together the adiabatically optimized in-solvent geometries for the monomer halves in their Ru(II) and Ru(III) oxidation states obtained in Step B, as illustrated in Fig. 1. We then

evaluate, using appropriate multi-reference methods, the vertical excitation energies Δ_e and Δ_n for the electronic transition from an initial electronic structure (say Ru(II)–Ru(III)) to a final one (thence Ru(III–Ru(II)), both with full equilibrium solvation (Δ_e) and with non-equilibrium solvation (Δ_n). The full-equilibrium solvation calculation is in fact a usual SCRF calculation whilst in the non-equilibrium one the static component of the dielectric response is frozen at its initial-state value and only the high-frequency component is allowed to come into equilibrium with the final electronic state. This later quantity can be evaluated with the initial state as either the ground state, thus evaluating the solvent effect pertaining to absorption Δ_n^A, or the excited state, thus evaluating the solvent shift pertaining to emission Δ_n^E. Whilst in general significantly different responses for absorption and fluorescence are expected (cf. Eq. (1)), for symmetric charge-transfer systems very similar values are actually expected (differences arise mainly from the differing polarizabilities of the two states [33] and the symmetric-mode displacements). We find that the prediction of very similar responses for absorption and emission is a necessary criterion for determining the stability of the computational method used, and consider thenceforth mainly the average solvent effect

$$\Delta_n = \frac{\Delta_n^E + \Delta_n^A}{2}. \tag{3}$$

As the quantum-chemical calculations of Step D are performed using the Born–Oppenheimer adiabatic approximation, it is valid to use adiabatic theory to interpret their results in terms of a fusion of the desired solvent reorganization energies with the inherent coupling J present within the dimer. The calculated solvent effects thus correspond to

$$\Delta_e = (\lambda_a^2 + 4J^2)^{1/2}, \tag{4}$$

and

$$\Delta_n = (\lambda^2 + 4J^2)^{1/2}, \tag{5}$$

hence as the electronic coupling J is evaluated in Step A it is possible to evaluate both λ_a and λ_e as $\lambda = \lambda_a + \lambda_e$. Step D thus provides an independent estimate of λ_a than that obtained in Step C; the differences found between these independent estimates provides a measure of the reliability of aspects of the computational procedure.

For the Creutz–Taube ion it is clear beforehand that $2|J|$ and λ are of the same order, however, and hence the application of these adiabatic equations would take a central position in the final analysis. For example, it could be possible that non-Condon effects concerning the variation in J with antisymmetric displacements are important [81]. In this case, Step A could be modified to use methods such as GMH to provide a more appropriate estimate of J [51]. Our emphasis in this work is on avoiding such issues by using a modification of the basic method in Step D. It is specific to ruthenium-type systems and utilizes the known property that the metal centres have each three t_{2g} orbitals that are essentially equivalent in terms of the solvent reorganization energy associated with their oxidation yet very different in terms of their through-bridge coupling. In symmetric dimers, one strongly interacting pair, the d_π pair, interact directly with the π orbitals of the bridge, forming the deepest-lying and highest-lying t_{2g} orbitals of the dimer. The other two pairs are oriented away from the bridge and are non-bonding in nature and hence possess nearly negligible interaction energies. We thus apply Step D not to evaluate the effects of oxidation from d_π but rather for oxidation involving an alternate set named d_n whose (weak) electronic coupling is denoted by J_n and is evaluated in addition to the primary coupling J using the appropriate modification to Step A.

3. Quantum-chemical methods

The a priori method in most common use for the evaluation of the properties of charge-transfer systems is density-functional theory (DFT). In particular, DFT has been shown to predict electronic couplings J of the correct order for the Creutz–Taube ion **1**, and we apply it to determine J, λ_s, and λ_a for it and its dipyridyl analogue **2**. Specifically, the B3LYP density functional [82] is used to evaluate the energies for Steps A and B in conjunction with the 6–31G* basis set [83] for H, C, and N and the SDD basis set [84] for Ru using the GAUSSIAN-03 [47] computational package. With this package, calculations including correction for solvent were performed using the PCM model [85,86] for the SCRF. As calculations of this type are known to be sensitive to intramolecular geometries [77], we investigated a variety of computational methods and chose the one that provides the best agreement between calculated Ru–N distances and their observed values from X-ray scattering experiments. The method chosen was the electrostatic-potential (ESP) point-charge SCRF approach [87] as implemented in the JAGUAR [88] computational package; the B3LYP density functional and the 6–31G* basis set were again used, but the LANL2DZ basis set [89] was used for Ru instead of SDD; some gas-phase geometry optimizations were also performed using the SDD basis set by GAUSSIAN-03.

All modern functionals used in DFT calculations possess a number of established [90] systematic weaknesses and not all conceivable calculations of charge-transfer phenomena are expected to yield reliable results. Steps A and B are well-suited to DFT calculations as they involve only the determination of energies of the ground state of specific spin and orbital symmetries. However, DFT predicts poor results for extended

conjugated systems as it systematically underestimates molecular band gaps and this effect becomes critical when the actual band gap gets small. In particular, DFT does not produce a closed-shell singlet ground state for polyacetylene [91] and predicts that, for the series of compounds **2**–**4**, the coupling magnitude $|J|$ starts to increase with increasing bridge length, contrary to the observed exponential decay [92]. Also, Step D requires unavoidably the evaluation of energies for excited electronic states of the same symmetry as the ground state. The most common method in use for the application of DFT to such problems is time-dependent DFT (TDDFT). This, however, is a method based on a single-reference expansion of the excited states. Such methods do not provide the flexibility necessary to properly describe the core electrons in charge-transfer excited states, and lead necessarily to poor descriptions of the excited state manifold. Indeed, TD-DFT, like related methods such as both ab initio and semi-empirical single-excitation CI procedures, is known to produce erratic results for charge-transfer transitions [93]. Hence TD-DFT is inappropriate for use in Step D.

Only multi-reference methods may robustly describe charge-transfer excited states of the same symmetry as the ground state [35] as is required during Step D; we apply the complete-active-space self-consistent field (CASSCF) computational method using the MOLCAS program package [48]. Multi-reference DFT-based approaches are becoming available (see eg. DFT-MRCI [94]) as an alternative, approaches that are expected to be in general more quantitative than is CASSCF. Also, it may be possible to complete the required calculations as two independent DFT calculations, one for each surface. While this is in general not possible for molecular states of the same symmetry, strong solvent–solute interaction can facilitate it, see later. However, closely related methods to CASSCF are known to predict the correct bridge-length dependence for the electronic coupling J in the α,ω-dipyridyl polyene analogues of the Creutz–Taube ion including molecules **2**–**4** [92], an important property that is poorly described using DFT, and hence we choose the more conservative CASSCF procedure in this work.

In the CASSCF calculations, the 6–31G* basis set [83] for H, C, and N and the SDD basis set [84] for Ru are again used, along with the PCM method [85,86] for treatment of the solvent SCRF. The MOLCAS program package was modified in one small but highly significant way: a radius of 3 Å was set for Ru in the SCRF calculations, sufficient to prevent dielectric penetration within the inner ligand shell and in so doing dramatically stabilize the calculations. The active space consisted of three electrons distributed in the two d_n orbitals. To achieve such an active space (in general 11 electrons in the 6 t_{2g} orbitals would be required), the molecular geometry was chosen such that the two d_n orbitals were located in the bridge π plane with a′ symmetry whilst the remaining four fully occupied t_{2g} orbitals have a″ symmetry and hence can be eliminated from the active space without further approximation. In addition, molecules **2**–**4** were constrained to have planar ligands in order to achieve the required point group symmetry. While deviations from planarity caused by steric repulsions between hydrogen atoms have significant quantitative effects in reducing J [92], these are not expected to influence the solvent reorganization energy λ_e, the quantity of primary interest herein.

Completion of the CASSCF calculations is not straight forward, however, due to some unique technical difficulties that arise for this system. During the evaluation of properties for excited states of the same symmetry as the ground state, it is usual in CASSCF calculations to perform a ''state averaged'' calculation in which the peripheral orbitals are optimized to minimize the average energy of both the ground and excited states. As shown in Fig. 1, these two states have opposing charge distributions and state averaging will thus result in the charge being equally shared by both metal atoms. This will take the system out of the intended localized diabatic regime so that the resultant energies do not have the required physical interpretation. In principle, this problem can be overcome by using uneven weighting of the two states such as 95% excited state with 5% ground state, hence causing only 10% charge delocalization. However, MOLCAS evaluates only one reaction field, applying it to both states. As solvation of the excited state stabilizes it with respect to the ground state to the point that it itself becomes the ground state, the program is incapable of locking onto the desired solution making such calculations non-convergent. To overcome this problem, a scheme was devised in which the gas-phase excited state was stabilized to become the ground state through the application of a point charge of $-0.2e$ at a distance of 5 Å behind the metal centre of valence Ru(II) in the ground state of the asymmetric dimer. The presence of this point charge stabilized oxidation of the nearby metal centre, hence reversing the energy ordering of the states. Care must be taken in order to prevent bridge oxidation during this process, however, by keeping the perturbation to a minimum. Next, the resultant orbitals were used in a configuration-only calculation without the external point charge in which the doubly occupied orbitals were frozen, locking the excited state in place so that the SCRF for this state could be evaluated. From the resulting orbitals and solvent reaction field, the full CASSCF calculation in solution was launched. This calculation remained locked on the excited state, MOLCAS being unable to determine that a lower-energy state exists as this requires the simultaneous relaxation of both the external orbitals and the reaction field whereas the program relaxes each part only sequentially. Hence a very

stable procedure was developed for determining the electronic structure and reaction field for the excited state. Interestingly, this final procedure involves essentially the mapping of an excited-state problem that is poorly suited to DFT onto a ground-state one for which it is well suited, and hence a reliable DFT implementation of Step D can now be envisaged.

4. Results

The bond lengths calculated for optimized structures in high symmetry both in the gas phase and with SCRF solvation using the ESP point-charge PCM model [87] are given in Table 1 for the 5+ oxidation states of the Creutz–Taube ion **1** and its 4,4′-bipyrimidyl analogue **2**. The results show that, in particular for the Creutz–Taube ion, there is a marked dependence of the optimized Ru–N bond lengths on both basis set and the inclusion of solvation corrections. For the Crautz–Taube ion, changing the Ru basis set from the small LANL2DZ one to the moderate sized SDD one causes the bond length to contract by 0.09–0.15 Å; similar effects have been previously found for this system [77]. Geometries that show proper convergence with respect to basis set expansion will thus be difficult to obtain. More striking, however, is the effect of solvation on the Ru–pyrazine separation, which brings about a 0.18 Å contraction for the ground state and a massive 0.39 Å contraction for the excited state. Similar effects on the metal–amine bond lengths are not found, however, and it thus appears that the solvent in fact acts to modify metal to pyrazine charge transfer, consistent with the notion that metal to ligand charge-transfer states are coupled to intervalence charge transfer [70–72]. It is hence clear that proper treatment of solvation is also essential in calculations of this type. Finally, while we do not consider variations in density-function nor the use of alternate methods, we note that these variations are known to produce significant effects [77,95].

Calculated couplings and reorganization energies obtained using Steps A–D are given in Table 2. As anticipated, the d_n orbitals interact very weakly, with coupling strengths in the region of $|J_n| = 1$–$260\ cm^{-1}$, while the primary electronic coupling for the d_π orbitals calculated for the Creutz–Taube ion is much larger at $|J| = 2400\ cm^{-1}$. Our results reproduce the previous findings [77] that J is very sensitive to geometry, with for example the corresponding quantity for the Creutz–Taube ion evaluated at the gas-phase optimized geometry being just $1450\ cm^{-1}$. Using similar methods it has been reported by Bencini et al. [77] at $3407\ cm^{-1}$ at the X-ray geometry. Their computational procedure, however, is now known [8,17] to yield not J but rather $|J| + \lambda_s/2$, and using our value of $\lambda_s = 630\ cm^{-1}$ from Table 2 this coupling reduces to $3092\ cm^{-1}$. The difference between this and our value of $2400\ cm^{-1}$ can be attributed primarily to our slight overestimation of the Ru–pyrazine bond length, although basis set differences may also be significant. From these results and those for other density functionals [77], as the relationship between the geometry in solution and in ionic crystals is not known, it appears that the best DFT estimate for the coupling in the Creutz–Taube ion is in the range 2400–$3600\ cm^{-1}$. For **2**, the calculated coupling is $|J| = 930\ cm^{-1}$, significantly greater than the observed value [14] of $390\ cm^{-1}$. This difference is partly due to neglect of out-of-plane distortion within the ligand, but the DFT bandgap error for extended conjugated system [90–92], an effect that is much more pertinent for 4,4′-bipyridine than it is for pyrazine, also contributes. The overestimation of the coupling for this ligand is thus not taken to indicate an expected overestimation of the coupling in the Creutz–Taube ion.

The calculated values of λ_a and λ_s vary significantly for **1** and **2**, and the values of λ_a for each molecule determined during Steps C and D differ markedly. This indi-

Table 1
Calculated[a] and observed[b] Ru–N bond lengths, in Å, for high-symmetry ground state and intervalence excited state structures of the 5+ valence states of the Creutz–Taube ion **1** and its 4,4′-bipyridyl analog **2**

Molecule	Bond	Ground state (^2B_g)				Intervalence excited state (^2A_u)		
		SDD gas phase	LANL2DZ gas phase	LANL2DZ ESP SCRF	Observed	SDD gas phase	LANL2DZ gas phase	LANL2DZ ESP SCRF
1	Pyrazine	2.166	2.257	2.079	1.97–2.00	2.417	2.567	2.182
	trans NH_3	2.185	2.180	2.154	2.12–2.14	2.148	2.145	2.142
	Average *cis* NH_3	2.192	2.204	2.168	2.11	2.191	2.202	2.159
2	4,4′-Bipyridine	2.147	2.180	2.109		2.202	2.222	2.146
	trans NH_3	2.196	2.203	2.165		2.186	2.197	2.161
	Average *cis* NH_3	2.188	2.201	2.170		2.187	2.201	2.165

[a] Obtained using the B3LYP density function with the 6–31G* basis set for H, C, and N and either the SDD or LANL2DZ basis set for Ru, for molecules either in the gas phase or subject to the ESP SCRF solvation model [87].
[b] From [61].

Table 2
Calculated and observed properties of the Creutz–Taube ion and its dipyridyl polyene analogues

Molecules	R (Å)	Dimer in C_{2h} symmetry[a]			Monomer[b]	Difference[c]	Dimer in C_s symmetry[d]							Observed[e]		
		$\lvert J_n\rvert$	$\lvert J\rvert$	λ_s	$\lambda_s+\lambda_a$	λ_a	Δ_e	λ_a	Δ_n^A	Δ_n^E	Δ_n	λ	λ_e	$h\nu$	$\lvert J\rvert$	λ
1	7.2	260	2400	630	1230	600	1050	1020	6290	6060	6175	6170	5150	6350		
2	11.5	21	930	100	200	100	1020	1020	8760	8820	8790	8790	7770	9200	390	9170
3	13.8	3					1016	1016	9500	9460	9480	9480	8464	9900	300	9880
4	16.1	0.7					1014	1014	10,110	10,050	10,080	10,080	9066	10,500	215	10,490

[a] Step A, from total energies in cm^{-1} evaluated B3LYP/6–31G*/SDD for J and λ_s and CASSCF/6–31G*/SDD for J_n, all obtained using the PCM solvent model at the appropriate geometry optimized using B3LYP/6–31G*/Lanl2DZ using the ESP SCRF solvation model [87].
[b] Step B, from total energies in cm^{-1} evaluated B3LYP/6–31G*/SDD using the PCM solvent model for the appropriate monomeric ruthenium complexes in their Ru(II) and Ru(III) oxidation states at their geometries optimized B3LYP/6–31G*/Lanl2DZ using the ESP SCRF solvation model [87].
[c] Step C, the difference of quantities from Steps A and B.
[d] Step D, from CASSCF/6–31G*/SDD total energy differences in cm^{-1} obtained using the PCM solvent model at the low-symmetry geometry for the dimer obtained by splicing geometries (see Fig. 1) optimized for each individual monomer half using B3LYP/6–31G*/Lanl2DZ and the ESP SCRF solvation model [87].
[e] Observed band centre $h\nu$ in cm^{-1} from [1–5]; for the dipyridyl polyenes, the values of J and λ are determined [14] from experimental data using adiabatic equations, including Eq. (4), appropriate for the localized diabatic limit.

cates that not all the computational methods used are reliable for these properties. It arises from the strong dependence of the dominant term, the electronic coupling J, on the Ru-bridge bond length. Steps A–C have proven reliable in other applications in which the charge is delocalized over a macrocyclic ring [8], however, as for such systems the solvent does not significantly perturb the intramolecular structure. The seemingly consistent variation in λ_a in the region of 1014–1020 cm^{-1} obtained using Step D based on asymmetric structures suggests that this method may produce realistic answers while the more orthodox approaches typified by Steps A–C do not. Invariance of λ_a to the bridging ligand indicates that the vibronic coupling with the metal is dominated by metal–nitrogen vibrational modes and is insensitive to the relatively small changes that occur to the vibrations of the central bridge molecule.

Indeed, Table 2 shows that for all calculated properties, Step D returns values that reveal the anticipated subtle changes associated with increasing the length of the polyene spacer through molecules **2**–**4**. For these molecules it is established that $2|J|/\lambda \ll 1$ and hence adiabatic theory [54] may be applied to extract $|J|$ and λ from the observed data, and the results [14] are also given in the Table. As Eq. (2) suggests that the external contribution to λ scales as $1/R$, we plot in Fig. 2 the calculated and observed values of λ as a function of this variable, including also the line of best fit through the calculated data. The slope of this line is given in Table 3 as $-d\lambda/dR^{-1} = 0.451$ in dimensionless atomic units, while the intercept of this line is represented assuming a constant $\lambda_a = 1016\ cm^{-1}$. This leads to the identification of an "effective radius" of the donor and acceptor groups $r_A = r_D$ as 4.26 Å from Eq. (2). The results for similar analyses performed on the calculated data for molecules **2**–**4** only, and on the observed data for these

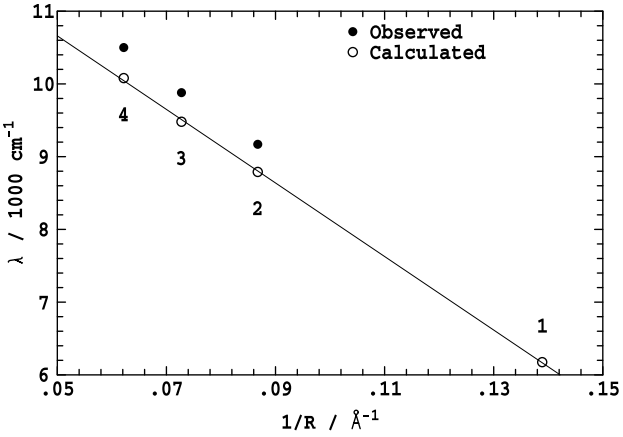

Fig. 2. The observed and calculated reorganization energy λ from Table 2 plotted as a function of the reciprocal of the inter-metallic distance R for the Creutz–Taube ion **1** and its α,ω-dipyridyl polyene analogues **2**–**4**; the line of best fit to the calculated points is shown.

Table 3
Properties of the linear fits to the observed and calculated correlations of λ with $1/R$ obtained for the Creutz–Taube ion **1** and its α,ω-dipyridyl polyene analogues **2**–**4**

Method	$-d\lambda/dR^{-1}$	$r_D = r_A$ (Å)
Observed for molecules **2**–**4**	0.461	4.19
Calculated for molecules **2**–**4**	0.451	4.26
Calculated for molecules **1**–**4**	0.435	4.15
$1/n^2 - 1/\epsilon$	0.550	–
vdw Radius of $Ru(NH_3)_6$	–	3.44
vdw Radius of $Ru(NH_3)_5$ pyridine	–	3.75

molecules, are also given in this table. The observed and calculated slopes for **2**–**4** differ by less than the errors associated with the linear interpolation procedure indicating that the computational method quantitatively

reproduces the experimental results. The value of the slope expected from Eq. (2) using the values of $n^2 = 1.776$ and $\epsilon = 78.39$ used by MOLCAS is also shown in the table and is 20% higher than these values. The SCRF electronic structure calculations are thus interpreted as enhancing the original analytical model so as to establish quantitative accuracy. Also, D the radii r_D, etc., appearing in Eq. (2) are often associated with the radius of a sphere that contains the same volume as does the van der Waals surface of the fragments. These radii for ruthenium hexamine and ruthenium pentamine pyridyl model compounds are also given in Table 3 and are 20% and 10%, respectively, less than the radii that come from use of Eq. (2). It has been stressed that Eq. (2) is inadequate in that it does not take into account the simultaneous polarization of the medium by both the donor and acceptor charges, an effect suggested to essentially double the effective radius of the charges [46]. While the results from our a priori computational scheme that embodies these interference effects do suggest quantitative limitations of Eq. (2), the effect is not as great as expected [46]. Additionally, as is apparent from Fig. 2, the computed reorganization energies underestimate the observed ones by some 400 cm^{-1}, an effect which from Table 3 can be interpreted as arising from an error of 0.07 Å in size of the donor and acceptor groups as perceived by the PCM model. This error could simply be due to overestimation of the Ru–N bond lengths as depicted in Table 2.

5. Conclusions

A practical computational method has been introduced for the a priori evaluation of the solvent contribution to the reorganization energy driving charge localization in systems capable of sustaining electron-transfer reactions. It has been tested by comparison of predictions with known data for the α,ω-dipyridyl polyene analogues of the Creutz–Taube ion and shown to be quantitatively accurate. Previously, these contributions have only been accessible using simple analytical formulas such as Eq. (2); we demonstrate that this equation is indeed applicable to these systems but is quantitatively in error by 10–20% for key properties, and that its deficiencies are eliminated through the full numerical multi-reference electronic-structure computational approach.

A wide range of inorganic charge-transfer systems whose properties should throw more light on the characterization of systems in the maximum non-adiabatic regime is now being produced [55]. As typified by the Creutz–Taube ion, most effort in the theoretical prediction of such systems has been directed towards the evaluation of the electronic coupling J, and indeed on this basis the Creutz–Taube ion has been interpreted as being a fully delocalized system [77]. However, we demonstrate that J is very difficult to calculate reliably for inorganic systems as solvation dramatically alters the intramolecular structure. Hence proven methods for its evaluation in organic systems [78] become unstable in this context. Also, the significant dependence of J on basis set and on computational method for inorganic complexes adds to the unreliability of the approach, and the need for proper treatment of symmetric modes [8,16,17] has not until recently been fully appreciated with the result that previous interpretations of calculated data (e.g., see [77]) have inflated the driving force for delocalization.

A good model system for understanding the interrelationship between J,λ_s, and calculated vertical excitation energies is the nature of the localization/delocalization of the (n,π*) excitation over the two nitrogen atoms in the diazines pyrimidine, pyridazine, and pyrazine. Pyrimidine, for example, has a delocalized structure for its lowest (n,π*) excited state in the gas phase with a vertical excitation energy of 6300 cm^{-1} between the two electronic (n,π*) states [9], very similar to the energy difference in the Creutz–Taube ion. For pyrimidine, however, the weak solvent reorganization energy arising from Eq. (1) [96], or complexation with a single water molecule [97] that introduces an asymmetry of just ~1400 cm^{-1}, is able to induce full excitation localization on one nitrogen atom, and the weak internal reorganization energy λ_a is sufficient to place the gas-phase system near the maximum non-adiabatic coupling regime. In this case, the calculated vertical energy difference is dominated by the *symmetric-mode* reorganization energy, with proper estimates of J for this system being of order 0–900 cm^{-1}. While there are many close analogies between the Creutz–Taube ion and the excited states of pyrimidine, the major qualitative differences arise from the ratio of $|J|$ to λ_s *rather than to the usual* λ_a, and the greatly different magnitude of the dipole-moment change $\Delta\boldsymbol{\mu}$ on electron transfer which generates a much larger solvent reorganization energy λ_e for the Creutz–Taube ion.

These calculations have revealed new information that is crucial to the interpretation of the nature of the Creutz–Taube ion: the presumably reliable a priori prediction of a reorganization energy of $\lambda = 6170$ cm^{-1}, very close to the observed intervalence transition energy $h\nu = 6350$ cm^{-1}. This estimate is significantly larger than that of 3880 cm^{-1} coming from simpler interpretations of the absorption band width and temperature dependence [59,67] that deduce $2|J|/\lambda = 1.7$. While adiabatic approaches such as Eqs. 3, 4 deem that when $h\nu \sim 2|J|$ the system is delocalized (see. e.g. Bencini et al. [77] for an application of this logic) and when $h\nu \sim \lambda$ the system is localized, in the non-adiabatic regime these approaches do not actually apply and numerical simulations [16] indicate that when $2|J|/\lambda \sim 1$, the transition energy is more like $h\nu \sim 2|J| \sim \lambda$. Hence, for the

first time, a priori calculations clearly show that the Creutz–Taube ion is indeed a system for which $2|J|/\lambda \sim 1$, and are not inconsistent with the provocative postulate of Demadis, Hartshorn, and Meyer [55] that $2|J|/\lambda$ is actually less than 1. Recent interest in the properties of mixed-valence systems with similar properties has stemmed from their analysis.

Further progress in the a priori description of the nature of the Creutz–Taube ion requires most importantly the development of methods to predict stable, accurate values for the electronic coupling J and its dependence on symmetric vibrational displacements as well as its dependence on solvation. The experimental determination of Ru–N bond lengths in solution would greatly aid this process as for these complexes in particular solid-state values obtained from X-ray data may not properly represent the state of the molecule in solution. Once this is obtained, full non-adiabatic simulations of all chemical and spectroscopic properties need be performed, simulations that take into account all interacting electronic states and all active symmetric and antisymmetric vibrations. While in the past such simulations [8,16,17,75,76,98,99] have captured some of these aspects, the full quantum representation of the problem [8,16,17], the significance of the strong dependence of the electronic interaction on the symmetric modes, and computational methods for dealing with multi-state very-high mode problems (e.g., 4 states and 70 modes [18]) have only recently become available.

Improved methods for determining the solvent contribution to the reorganization energy beyond the CASSCF-based scheme presented herein can also be envisaged, either through the addition of perturbation theory to include electron correlation or through use of DFT. While Step D was originally thought unsuitable for reliable DFT application, the final method presented is couched in a way to make this a realistic proposal as it involves well-defined separate DFT calculations for the ground and excited states of the system. However, the strength of the computational scheme presented here is due to the basic simplicity of the quantities involved, as indicated by the quality of the results predicted by Eq. (2). As long as the electronic structure method used produces the chemically correct electronic structure for the complex, the main features controlling λ_e are geometric and are properly reproduced at most levels of electronic-structure theory. Hence, while the computational procedure developed contains many intricate steps and requires careful inspection to verify that each has been properly completed, the results are expected to be reasonably independent of the actual electronic-structure method, making the technique intrinsically highly reliable. This scenario could change if different specific solvation effects are operative for the initial and final states involved, or if the molecular structure of the solvent changes considerably on excitation [28,33,34,100,101], and both improved SCRF [34] and general methods utilizing explicit solvent structures are available, if required, [22–27]. However, as strong hydrogen bonding interactions between the ammonia ligands and the solvent dominate the solvation process in *both* the initial and final electronic states of the Creutz–Taube ion, electron-transfer processes on the ruthenium centres do not give rise to significant short-range changes in the solvent structure [22,23] and hence simplistic dielectric-continuum models are appropriate. Lastly, a simplification of the computational procedure is to use the actual interacting d_π orbitals during Step D instead of the non-adiabatic ones used herein. This will require careful consideration of the method used for diabatization of the potential-energy surface in order to extract the most appropriate value of the coupling J, however.

It is interesting to note that, while great interest in inorganic charge-transfer systems is due to the fact that they provide simple models for complex biological systems, the methods applied herein to enable a priori computation of these systems were initially developed for classical aromatic organic spectroscopy [9,52,97] (e.g., the excited states of pyrimidine) and for the analysis of photosynthetic proteins [8,18,78,102]. Indeed, many examples of organic molecular excited states are known in which excitations can be either localized on one chromophore or delocalized over two, systems that have been well characterized both experimentally and theoretically in their various diabatic and non-adiabatic limits [7]. Protein environments, whilst once appearing intimidating in their complexity, now through techniques such as site-directed mutagenesis offer means of obtaining tight control over electrontransfer systems, allowing continuous tuning through the non-adiabatic region [18], making for example the bacterial photosynthetic reaction centre one of the best characterized examples of an electrontransfer system in the non-adiabatic regime so that *it* now provides a model system for the Creutz–Taube ion!

Acknowledgements

We thank the Australian Research Council for supporting this research and the Australian Partnership for Advanced Computing (APAC) for the provision of computational resources.

References

[1] C. Creutz, H. Taube, J. Am. Chem. Soc. 91 (1969) 3988.
[2] C. Creutz, H. Taube, J. Am. Chem. Soc. 95 (1973) 1086.
[3] J.E. Sutton, P.M. Sutton, H. Taube, Inorg. Chem. 18 (1979) 1017.
[4] D.E. Richardson, H. Taube, J. Am. Chem. Soc. 105 (1983) 40.

[5] S. Woitellier, J.P. Launay, C.W. Spangler, Inorg. Chem. 28 (1989) 758.
[6] M. Born, R. Oppenheimer, Ann. Phys. 84 (1927) 457.
[7] G. Fischer, Vibronic Coupling, Academic Press, London, 1984.
[8] J.R. Reimers, N.S. Hush, J. Chem. Phys. 119 (2003) 3262.
[9] G. Fischer, Z.-L. Cai, J.R. Reimers, P. Wormell, J. Phys. Chem. A 107 (2003) 3093.
[10] W.A. Shapley, J.R. Reimers, N.S. Hush, Int. J. Quant. Chem. 90 (2002) 424.
[11] Z.-L. Cai, J.R. Reimers, J. Phys. Chem. A 106 (2002) 8769.
[12] J.M. Hughes, M.C. Hutter, J.R. Reimers, N.S. Hush, J. Am. Chem. Soc. 123 (2001) 8550.
[13] J.R. Reimers, L.E. Hall, J. Am. Chem. Soc. 121 (1999) 3730.
[14] J.R. Reimers, N.S. Hush, Inorg. Chem. 29 (1990) 3686.
[15] J.R. Reimers, N.S. Hush, Inorg. Chem. 29 (1990) 4510.
[16] J.R. Reimers, N.S. Hush, Chem. Phys. 208 (1996) 177.
[17] J.R. Reimers, N.S. Hush, Chem. Phys. 299 (2004) 79.
[18] J.R. Reimers, N.S. Hush, J. Am. Chem. Soc. 126 (2004) 4132.
[19] J.R. Reimers, N.S. Hush, Chem. Phys. 134 (1989) 323.
[20] J.R. Reimers, N.S. Hush, J. Photochem. Photobiol. A 82 (1994) 31.
[21] J.R. Reimers, N.S. Hush, in: K. Prassides (Ed.), Mixed Valence Systems: Applications in Chemistry, Physics, and Biology, Kluwer Academic Publishers, Dordrecht, 1991, p. 29.
[22] N.S. Hush, J.R. Reimers, Chem. Rev. 100 (2000) 775.
[23] N.S. Hush, J.R. Reimers, Coord. Chem. Rev. 177 (1998) 37.
[24] I.V. Leontyev, M.V. Vener, I.V. Rostov, M.V. Basilevsky, M.D. Newton, J. Chem. Phys. 119 (2003) 8024.
[25] H. Sato, Y. Kobori, S. Tero-Kubota, F. Hirata, J. Phys. Chem. B 108 (2004) 11709.
[26] K. Kumar, I.V. Kurnikov, D.N. Beratan, D.H. Waldeck, M.B. Zimmt, J. Phys. Chem. A 102 (1998) 5529.
[27] K. Siriwong, A.A. Voityuk, M.D. Newton, N. Roesch, J. Phys. Chem. B 107 (2003) 2595.
[28] S. Gupta, D.V. Matyushov, J. Phys. Chem. A 108 (2004) 2087.
[29] P. Vath, M.B. Zimmt, D.V. Matyushov, G.A. Voth, J. Phys. Chem. B 103 (1999) 9130.
[30] I.V. Leontyev, M.V. Basilevsky, M.D. Newton, Theor. Chem. Acc. 111 (2004) 110.
[31] J. Tomasi, M. Persico, Chem. Rev. 94 (1994) 2027.
[32] L. Serrano-Andrés, B.O. Roos, J. Am. Chem. Soc. 118 (1996) 185.
[33] E.L. Mertz, E.D. German, A.M. Kuznetsov, Chem. Phys. 215 (1997) 355.
[34] M.V. Basilevsky, I.V. Rostov, M.D. Newton, Chem. Phys. 232 (1998) 189.
[35] J. Zeng, N.S. Hush, J.R. Reimers, J. Am. Chem. Soc. 118 (1996) 2059.
[36] M. Born, Z. Phys. 1 (1920) 45.
[37] L. Onsager, J. Am. Chem. Soc. 58 (1936) 1486.
[38] N.S. Bayliss, J. Chem. Phys. 18 (1950) 292.
[39] E.G. McRae, J. Phys. Chem. 61 (1957) 562.
[40] W. Liptay, Z. Naturforsch. Teil. A 20 (1965) 272.
[41] W. Rettig, J. Mol. Struct. 84 (1982) 303.
[42] R.A. Marcus, J. Chem. Phys. 24 (1956) 966.
[43] N.S. Hush, Trans. Farad. Soc. 57 (1961) 577.
[44] S.F. Nelsen, D.A. Trieber II, R.F. Ismagilov, Y. Teki, J. Am. Chem. Soc. 123 (2001) 5684.
[45] J. Zeng, N.S. Hush, J.R. Reimers, J. Chem. Phys. 99 (1993) 1508.
[46] K.-X. Fu, X.-Y. Li, Q. Zhu, Z. Gong, S.-Z. Lu, Z.-M. Bao, Theochem 715 (2005) 157.
[47] M.J. Frisch, G.W. Trucks, H.B. Schlegel, et al., GAUSSIAN-03 Rev. B2, Gaussian Inc., Pittsburgh, PA, 2003.
[48] K. Andersson, M. Barysz, A. Bernhardsson, M.R.A. Blomberg, D.L. Cooper, T. Fleig, M.P. Fülscher, C.d. Gagliardi, B.A. Hess, G. Karlström, R. Lindh, P.-Å. Malmqvist, P. Neogrády, J. Olsen, B.O. Roos, A.J. Sadlej, M. Schütz, B. Schimmelpfennig, L. Seijo, L. Serrano-Andrés, P.E.M. Siegbahn, J. Stålring, T. Thorsteinsson, V. Veryazov, P.-O. Widmark, Molcas Version 5, University of Lund, Lund, 2000.
[49] H.-J. Werner, B. Follmeg, M.H. Alexander, J. Chem. Phys. 89 (1989) 3139.
[50] D. Simah, B. Hartke, H.-J. Werner, J. Chem. Phys. 111 (1999) 4523.
[51] R.J. Cave, M.D. Newton, Chem. Phys. Lett. 249 (1996) 15.
[52] Z.-L. Cai, J.R. Reimers, J. Phys. Chem. A 104 (2000) 8389.
[53] G.C. Allen, N.S. Hush, Prog. Inorg. Chem. 8 (1967) 357.
[54] N.S. Hush, Prog. Inorg. Chem. 8 (1967) 391.
[55] K.D. Demadis, C.M. Hartshorn, T.J. Meyer, Chem. Rev. 101 (2001) 2655.
[56] B.S. Brunschwig, C. Creutz, N. Sutin, Chem. Soc. Rev. 31 (2002) 168.
[57] J.T. Hupp, Comprehensive Coord. Chem. II 2 (2004) 709.
[58] N.S. Hush, A. Edgar, J.K. Beattie, Chem. Phys. Lett. 69 (1980) 128.
[59] J.K. Beattie, N.S. Hush, P.R. Taylor, Inorg. Chem. 15 (1976) 992.
[60] S.P. Best, R.J.H. Clark, R.C.S. McQueen, S. Joss, J. Am. Chem. Soc. 111 (1989) 548.
[61] U. Fürholz, H.B. Burgi, F.E. Wagner, A. Stebler, J.H. Ammeter, E. Krausz, R.J.H. Clark, M.J. Stead, A. Ludi, J. Am. Chem. Soc. 106 (1984) 121.
[62] E. Krausz, C. Burton, J. Broomhead, Inorg. Chem. 20 (1981) 434.
[63] M.J. Powers, D.J. Salmon, R.W. Callahan, T.J. Meyer, J. Am. Chem. Soc. 98 (1976) 6731.
[64] H. Lu, V. Petrov, J.T. Hupp, Chem. Phys. Lett. 235 (1995) 521.
[65] N.S. Hush, Chem. Phys. 10 (1975) 361.
[66] J.R. Reimers, N.S. Hush, J. Phys. Chem. 95 (1991) 9773.
[67] N.S. Hush, NATO Adv. Study Inst. Ser., Ser. C 58 (1980) 151.
[68] R. Delarosa, P.J. Chang, F. Salaymeh, J.C. Curtis, Inorg. Chem. 24 (1985) 4229.
[69] N.S. Hush, ACS Symp. Ser. 198 (1982) 301.
[70] L.-T. Zhang, M.J. Ondrechen, Inorg. Chim. Acta 226 (1994) 43.
[71] A. Ferretti, A. Lami, M.J. Ondrechen, G. Villani, J. Phys. Chem. 99 (1995) 10484.
[72] H. Bolvin, J. Phys. Chem. A 107 (2003) 5071.
[73] D.H. Oh, S.G. Boxer, J. Am. Chem. Soc. 112 (1990) 8161.
[74] D.H. Oh, M. Sano, S.G. Boxer, J. Am. Chem. Soc. 113 (1991) 6880.
[75] C.H. Londergan, C.P. Kubiak, J. Phys. Chem. A 107 (2003) 9301.
[76] A. Ferretti, A. Lami, L.F. Murga, I.A. Shehadi, M.J. Ondrechen, G. Villani, J. Am. Chem. Soc. 121 (1999) 2594.
[77] A. Bencini, I. Ciofini, C.A. Daul, A. Ferretti, J. Am. Chem. Soc. 121 (1999) 11418.
[78] J.R. Reimers, W.A. Shapley, A.P. Rendell, N.S. Hush, J. Chem. Phys. 119 (2003) 3249.
[79] J.R. Reimers, J. Chem. Phys. 115 (2001) 9103.
[80] G. Herzberg, E. Teller, Z. Phys. Chem. 21 (1933) 410.
[81] M.D. Newton, Theo. Chem. Acc. 110 (2003) 307.
[82] A.D. Becke, J. Chem. Phys. 98 (1993) 5648.
[83] W.J. Hehre, R. Ditchfield, J.A. Pople, J. Chem. Phys. 56 (1972) 2257.
[84] D. Andrae, U. Haeussermann, M. Dolg, H. Stoll, H. Preuss, Theor. Chim. Acta 77 (1990) 123.
[85] G. Karlström, J. Phys. Chem. 92 (1988) 1315.
[86] J. Tomasi, M. Persico, Chem. Rev. 94 (1994) 2027.
[87] D.J. Tannor, B. Marten, R. Murphy, R.A. Friesner, D. Sitkoff, A. Nicholls, M. Ringnalda, W.A. Goddard III, B. Honig, J. Am. Chem. Soc. 116 (1994) 11875.
[88] Jaguar 3.5, Schrödinger Inc., Portland OR, 1998.
[89] P.J. Hay, W.R. Wadt, J. Chem. Phys. 82 (1985) 270, 284,299.

[90] J.R. Reimers, Z.-L. Cai, A. Bilic, N.S. Hush, Ann. N.Y. Acad. Sci. 1006 (2003) 235.
[91] Z.-L. Cai, K. Sendt, J.R. Reimers, J. Chem. Phys. 117 (2002) 5543.
[92] J.R. Reimers, N.S. Hush, J. Phys. Chem. A 103 (1999) 3066.
[93] D.J. Tozer, R.D. Amos, N.C. Handy, B.O. Roos, L. Serrano-Andres, Molec. Phys. 97 (1999) 859.
[94] A.B.J. Parusel, S. Grimme, J. Porph. Phthalo. 5 (2001) 225.
[95] J. Hardesty, S.K. Goh, D.S. Marynick, J. Molec. Struct. (Theochem) 588 (2002) 223.
[96] H. Baba, L. Goodman, P.C. Valenti, J. Am. Chem. Soc. 88 (1966) 5410.
[97] Z.-L. Cai, J.R. Reimers, J. Phys. Chem. A 109 (2005) 1576.
[98] S.B. Piepho, E.R. Krausz, P.N. Schatz, J. Am. Chem. Soc. 100 (1978) 2996.
[99] M.J. Ondrechen, J. Ko, L.T. Zhang, J. Am. Chem. Soc. 109 (1987) 1672.
[100] H.J. Kim, J.T. Hynes, J. Am. Chem. Soc. 114 (1992) 10508.
[101] D.V. Matyushov, J. Chem. Phys. 120 (2004) 7532.
[102] J.R. Reimers, W.A. Shapley, N.S. Hush, J. Chem. Phys. 119 (2003) 3240.